THE JOURNAL OF PHYSICAL CHEMISTRY Letters

Letter

pubs.acs.org/JPCL

Environment Polarity in Proteins Mapped Noninvasively by FTIR Spectroscopy

Joshua Manor,[†] Esther S. Feldblum,[†] Martin T. Zanni,*[,‡] and Isaiah T. Arkin*[,†]

[†]The Alexander Silberman Institute of Life Sciences, Department of Biological Chemistry, The Hebrew University of Jerusalem, Edmund J. Safra Campus, Jerusalem, 91904, Israel

[‡]Department of Chemistry, University of Wisconsin, Madison, Wisconsin 53706-1396, United States

ABSTRACT: The polarity pattern of a macromolecule is of utmost importance to its structure and function. For example, one of the main driving forces for protein folding is the burial of hydrophobic residues. Yet polarity remains a difficult property to measure experimentally, due in part to its nonuniformity in the protein interior. Herein, we show that Fourier transform infrared (FTIR) linewidth analysis of noninvasive 1-^{13}C=^{18}O labels can be used to obtain a reliable measure of the local polarity, even in a highly multiphasic system, such as a membrane protein. We show that in the Influenza M2 H^+ channel, residues that line the pore are located in an environment that is as polar as fully solvated residues, while residues that face the lipid acyl chains are located in an apolar environment. Taken together, FTIR linewidth analysis is a powerful, yet chemically nonperturbing approach to examine one of the most important properties in proteins: polarity.

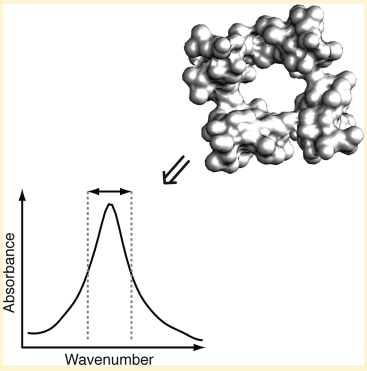

SECTION: Biophysical Chemistry

Most macromolecules are characterized by the fact that, while parts of the molecule are accessible to the polar solvent, others are not. In proteins, the particular polarity pattern is of critical importance to the structure and function of the molecule. For example, the burial of hydrophobic residues was already recognized in 1938 to represent the dominating factor in the folding of water-soluble proteins.[1,2]

Polarity in membrane proteins represents a further complication, due to the multiphasic environment of the lipid bilayer. In this regard, a particular residue might face the protein core, the polar headgroup region of the membrane, the apolar lipid acyl chains, an internal aqueous channel, or the external solvent, all without exclusivity. Taken together, the internal polarity of a protein is highly nonuniform[3] and can be substantially influenced by external factors.[4]

Currently, there are several approaches to investigate local polarity in proteins: Fourier transform infrared (FTIR) spectroscopic analysis of cyano[5] or azido[6−10] groups was shown to provide insight into the local electrostatic environment of the probes. Similarly, insertion of *p*-cyanophenylalanine was used to report on the local polarity using fluorescence spectroscopy.[11−13] Finally, measuring pK_a shifts of ionizable groups in protein interiors can provide information about the local electrostatic environment.[14] Yet, all of the aforementioned methods involve the potentially deleterious chemical modification of the protein under investigation. By contrast, we propose a different approach based on IR spectroscopic analysis of isotopically labeled proteins that is chemically neutral and, hence, nonperturbing.

We have previously shown the utility and ease in which the 1-^{13}C=^{18}O label may be used to derive structural properties at a unique position in a protein using FTIR spectroscopy.[15−25] The frequency of the isotope-edited peak is indicative of its secondary structure, while the dichroic ratio represents the bond-vector orientation.[26]

Previously, however, in order to derive information regarding the polarity of the labeled site, we would turn to 2D-IR spectroscopy, where we found a correlation between polarity and the homogenous linewidths.[27−29] Herein, we show that FTIR spectroscopy, a far simpler and widely accessible technique, under many circumstances can provide the same information using straightforward linewidth measurements, thereby dramatically increasing the applicability of our findings.

The system we investigated is the Influenza A M2 protein, a 97 amino acid, homotetrameric H^+ channel,[30,31] that serves as the target for the antiflu channel blockers amantadine and rimantadine.[32] Given that the transmembrane segment of the protein (residues S22-L46) is necessary and sufficient to promote channel activity and drug binding,[33,34] all discussion henceforth will concern this section of the protein.

Nine different peptides encompassing the transmembrane domain of the influenza M2 H^+ channel were used in the study. Each peptide contained a single 1-^{13}C=^{18}O label at a unique position, as indicated in Figure 1a. The peptides were purified, reconstituted in hydrated lipid bilayers and examined by FTIR spectroscopy at low pH, conditions in which the channel is known to be open.[30] Individual spectra alongside the fitted

Received: February 6, 2012
Accepted: March 12, 2012
Published: March 12, 2012

 © 2012 American Chemical Society

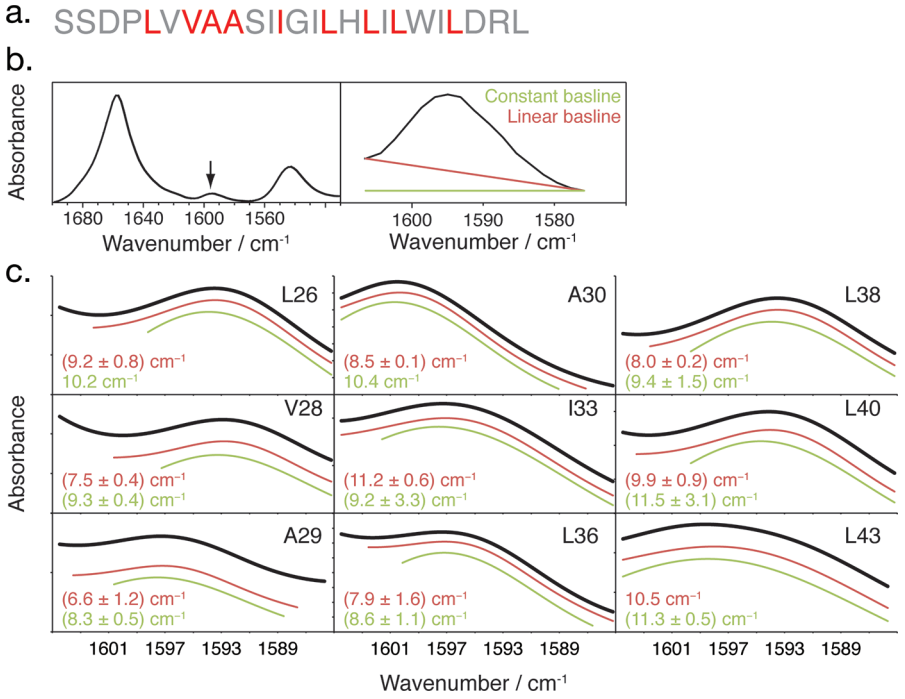

Figure 1. (a) Sequence of the transmembrane peptides of the Influenza A M2 channel (S22-ĐL46) used in the current study. The red coloring points to the location of the 1-^{13}C═^{18}O labeled amino acids. (b) Left panel: FTIR spectra of the M2 transmembrane peptide in hydrated lipid bilayers. The protein contains a single 1-^{13}C═^{18}O label at residue G34, which results in the isotope edited peak marked by an arrow. Right panel: Expansion of the spectra of the isotope edited peak depicting the two extreme possibilities for the baseline estimation. The linear baseline is depicted in red, while the constant baseline is shown in green. (c) FTIR spectra (black) in the region of the 1-^{13}C═^{18}O isotope edited amide I mode of the M2 transmembrane peptides in hydrated lipid bilayers. Each panel presents the spectrum of a peptide that contains a single 1-^{13}C═^{18}O label at the indicated position. Peak fits (vertically shifted for visual clarity) according to the linear or constant baseline, as well as the resulting linewidth values, are shown in red or green, respectively.

peaks are presented in Figure 1c. The resulting linewidths (full width at half-maximum) of the nine different isotope edited amide I modes are shown as red bars in Figure 2a.

Interestingly, the linewidths of the different amide I modes exhibit significant variation, ranging from less than 7 cm^{-1} to more than 11 cm^{-1}. The linewidth pattern is found to be independent of the vertical position of the labeled site in the helical bundle, as residues at the extremities (e.g., L26) exhibit the same linewidth as some residues in the middle of the membrane (e.g., I33). Moreover, the linewidth variation is clearly not dependent on the local secondary structure, since this segment of the protein is entirely α-helical.[35−38]

In order to gain insight into whether the local polarity of the protein is correlated with the FTIR linewidths, we made use of explicit molecular dynamics (MD) simulations. In brief, the X-ray structure of the same M2 transmembrane peptide[35] was used to construct a hydrated membrane−protein system, as described elsewhere in detail.[39−41] We then followed by measuring the time-averaged radial density of polar atoms in a 12 Å sphere around the labeled site, and depicted the results in Figure 2a (blue line). There exist more complicated methods of calculating infrared linewidths from MD simulations,[42−45] but the polarity contains the most essential component, which is the strength of the interaction between the solvent and peptide backbone.

Together, we could now show that the polarity of individual residues correlated closely (ρ = 0.83 and p < 0.3%) with their respective amide I mode linewidths, as seen in Figure 2a (blue line and red columns, respectively). It is important to note that the close correlation is evident irrespective of the lateral position of the labeled site. In other words, polarity and FTIR linewidths correlate well, both in residues in the peptide extremities, as well as for amino acids in the interior of the protein.

As stated above, we have previously examined the infrared linewidths of isotopically labeled transmembrane peptides using two-dimensional infrared (2D IR) spectroscopy.[25,27−29] In these studies, we found that the inhomogeneous linewidths of the amide I mode are correlated to their solvent accessibility. In contrast, the homogeneous linewidths showed little variation from site to site, and the variation in vibrational lifetime did not significantly contribute to linewidth variations. Semiclassical line shape theory reveals that the inhomogeneous linewidth variation is caused by the electrostatic disorder of the surrounding environment, which is not only due to water, but ions, lipids headgroups, and the peptides themselves.[47] Finally, other studies in the literature have also reported the sensitivity of the amide I mode to the environment, especially hydration, which is consistent with our results about polarity.[42−45]

Herein we show that the relative character of the FTIR linewidths can be interpreted in the same manner as the inhomogeneous linewidths measured by 2D IR spectroscopy. The reasoning behind this finding is that the homogeneous and vibrational lifetimes do not vary enough from site-to-site to significantly alter the total infrared linewidths. Hence, it is the homogenous component that is the main governing factor of the variation in the FTIR linewidths. Therefore, in principle, one does not need to separately measure the homogeneous and

dx.doi.org/10.1021/jz300150v | J. Phys. Chem. Lett. 2012, 3, 939−944

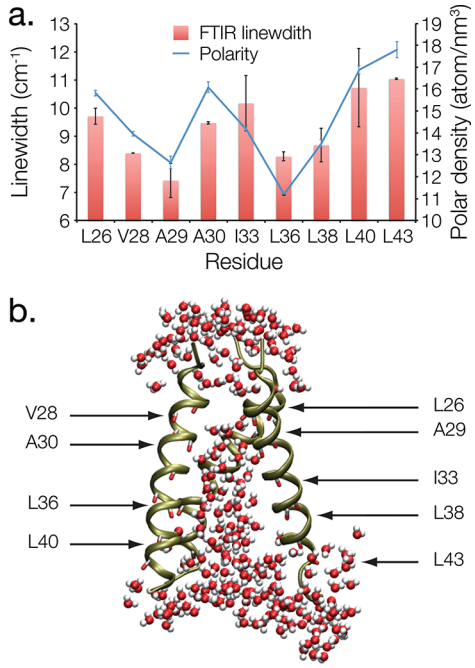

Figure 2. (a) FTIR full width at half-maximum linewidths (red columns) of nine 1-^{13}C=^{18}O amide groups in the influenza M2 H^+ channel, obtained in hydrated lipid bilayers.[25] The error bars are calculated as detailed in the Experimental section. Environment polarity (blue line) was measured as the time-averaged density of polar atoms in a 12 Å radius sphere about the geometric center of the respective C=O group during the course of a 20 ns MD simulation. The error bars represent the standard deviation of the atom density with respect to time in 2 ns bins. (b) Simulation snapshot of the M2 H^+ channel in hydrated lipid bilayers. The protein is shown in ribbon form, alongside the isotopically labeled 1-^{13}C=^{18}O residues (indicated in licorice). Any water molecules that are within 4 Å of the protein are depicted in CPK representation. One of the helices was removed for visual clarity. The image was produced using VMD.[46]

inhomogeneous linewidths with 2D IR, but instead only measure the total linewidth with FTIR.

Another potential difference between FTIR and 2D IR spectroscopy is background absorption. FTIR intensities scale as $c|\mu|^2$, whereas 2D IR intensities scale as $c|\mu|^4$, where c is the concentration and μ is the transition dipole strength. As a result, strong oscillators are enhanced relative to weak ones in 2D IR spectra, which largely eliminates nonspecific absorptions, such as solvent and side chain absorbance, and makes it more straightforward to extract linewidths. In FTIR spectroscopy, the nonspecific absorptions create a background, which makes the baseline less well-defined. Due to this uncertainty, we fit the FTIR linewidths using two extremes for possible baselines and found that both produced the same linewidth trend (see error ranges in Figure 2a red bars). We note that deconvolving the isotope edited peak by subtraction of an unlabeled sample is very difficult due to inconsistencies in the protein to lipid ratios of both samples.

Since the trends in FTIR linewidth match that of the 2D IR linewidths and MD derived polarity, we establish that FTIR spectroscopy can be used as a sensitive probe of environmental polarity. Since FTIR spectroscopy is a widely accessible experimental technique, our methodology is relevant to the general scientific community.

After having established the correlation between the FTIR linewidths and local polarity, it is informative to examine the results in detail. As expected, based on the conical frustum structure of the M2 protein,[35] the C-terminal residues are extensively solvated (see Figure 2b for a representative snapshot), and hence are located in a highly polar environment. This in turn, is reflected by the broader FTIR linewidths in residues L40 and L43. By contrast, residues that face the hydrophobic acyl chains of the lipid bilayer (e.g., A29 and L36) are located in an apolar environment and therefore, exhibit narrow FTIR linewidths. More interestingly, however, is the examination of the polarity of residues that face the channel lumen (e.g., A30 and I33). In this instance, the polarity as indicated by the FTIR linewidths is similar to that in the peptide extremities, or in other words, to fully solvated residues. Hence, our results suggest that in the M2 protein, the channel lumen is as polar as the bulk solvent.

In conclusion, we show that FTIR linewidths and solvent polarity correlate, and reveal that a channel lumen's polarity is similar to that of bulk solvent. Moreover, our results indicate that linewidths can be extracted from FTIR data that reflect the most structurally indicative measure of solvent polarity, which is the inhomogeneous linewidth. One should keep in mind that variations in the homogeneous and vibrational lifetimes, which would not be readily apparent in FTIR spectra, may alter the results, thereby requiring 2D IR spectroscopy. However, the correlation that we have found between polarity and FTIR linewidths holds true for most residues in all systems that we have so far investigated, including transmembrane helical peptide bundles with and without a water pore and surface bound helical polypeptides.[25,27−29] Finally, an inherent limitation of the approach is the reliance on 1-^{13}C=^{18}O isotopic labels. While incorporating such labels in synthetic peptides is trivial, it does require more sophisticated approaches to incorporate them in larger protein systems.[48]

It is also interesting that such a simple parameter as polarity can qualitatively reproduce the infrared linewidths as compared to the semiclassical and line shape theories used previously. We suspect this is because the polarity arises primarily from the water, which is also the most dynamic component of the system.[47] In conclusion, we show that the utility of non-perturbing isotopic amide I labels is not limited to the few researchers with access to 2D IR spectrometers, but can be applied by anyone with a widely available standard FTIR spectrometer.

EXPERIMENTAL SECTION

Peptide Synthesis. All peptides used in the current study encompass the transmembrane domain of the influenza A M2 channel and correspond to residues S22 to L46: SSDPLVVAA-SIIGILHLILWILDRL.[34] Peptide synthesis entailed standard solid-phase N-(9-fluorenylmethoxycarbonyl) chemistry, whereby 1-^{13}C=^{18}O labels were introduced as labeled amino acid precursors during the synthesis. The synthesis of the 1-^{13}C=^{18}O labels is described elsewhere in detail.[19,20]

Peptide Purification. Crude synthetic peptides were purified in a 20 mL Jupiter 5 C4-300 Å high performance liquid chromatography column (Phenomex, Cheshire, UK). The injected amount was 0.5 mg of the crude synthesis dissolved in 0.75 mL of trifluoroacetic acid. The column was pre-equilibrated with 80% H_2O, 8% (w/v) acetonitrile, and 12% (v/v) isopropanol. Finally, the peptide was eluted off the column with a linear gradient to a final solvent composition of 60% isopropanol and 40% acetonitrile. 0.1% (v/v) trifluoro-acetic acid was present in all solvents.

dx.doi.org/10.1021/jz300150v | J. Phys. Chem. Lett. 2012, 3, 939−944

Peptide Reconstitution. One milligram of peptide and 10 mg of 1,2-dimyristoyl-*sn*-glycero-3-phosphocholine (Avanti Polar Lipids, Alabaster, Al) were dissolved in 1 mL of 1,1,1,3,3,3-hexafluoro-2-propanol (Merck, Whitehouse Station, NJ). The solution was then warmed to 37° for 2 h. Following overnight desiccation, liposomes were prepared by dissolving the sample in 2 mL of water. Sonication (probe-type sonicator for 2 min at 100 W) and extrusion through 0.2 μm nitrocellulose filters ensured liposome homogeneity.

FTIR Spectra Collection. Attenuated total internal reflection (ATR) spectra were measured with a 25-reflection ATR accessory from Graseby Specac (Kent, England) on a Nicolet Magna 560 spectrometer (Madison, WI), equipped with a high-sensitivity liquid nitrogen-cooled MCT/A detector.

Approximately 0.5 mg/mL protein and 5 mg/mL lipid in 600 μL of sample were deposited onto a trapezoidal Ge internal reflection element (50 × 2 × 20 mm) under a stream of CO_2 and water-depleted air. The sample was adjusted with HCl to reach pH 4, which corresponds to the open form of the channel.[30]

The instrument was purged with CO_2 and water-depleted air, after which 1000 interferograms were collected and averaged for every sample. Spectra were processed with 1-point zero filling and Happ-Genzel apodization.

Linewidth Measurements. The isotope edited peak partially overlaps the "natural-abundance" 1-^{12}C=^{16}O amide I mode and other nonspecific weak absorbances. Therefore, in order to properly measure its linewidth, peak fitting is required with the appropriate baseline. Two extreme cases were considered, as shown in Figure 1b: (i) The peak sits entirely on the margins of the natural-abundance peak (linear baseline, red curve); (ii) Complete separation is assumed and the baseline is a straight line from one end of the peak to the other (constant baseline, green line).

Subsequently, the isotope edited peak was fit using the OMNIC FT-IR software (Nicolet, Madison, WI) with the line shape for both baseline extremes assuming a Voigt profile due to the following reasoning: Amide I vibrations are influenced by the surrounding environment. According to the central limit theorem, the distribution function of the frequency of these vibrations follows a Gaussian profile. The line shape function (or linear absorption spectrum) is proportional to the Fourier transform of the correlation function of the Gaussian profiles at time t = 0 when excitement occurs and at time t when measurement occurs. In the homogeneous limit, frequency fluctuations are rapid, or are of small amplitude. This is due to slow internal motions in this limit, and thus the time-scale of dephasing is greater compared to the time-scale of correlation. The spectrum measured, therefore, nears a delta function about the frequency dictated by the bond vector irrespective of its equilibrium phase. The line shape of this limit appears as a Lorentzian profile. In the inhomogeneous limit, frequency fluctuations are slower, or of greater amplitude, resulting from fast internal motions, lending to the time-scale of dephasing to be quicker (smaller) than the time-scale of correlation. This is exhibited by a Gaussian profile since a significant portion of the bond vectors are dephased by the time the measurement occurs. Biological systems generally exhibit both time-scales of internal motion, resulting in the convolution of the two line shape functions to yield a Voigt profile.

Finally, the full width at half-maximum linewidths of both peaks were then measured and averaged yielding the desired linewidth and standard deviation. The error bars represent the standard deviation of at least two spectra and include the two extreme baseline assumptions stated above. Note that the spectrometer resolution (2 cm^{-1}) was not taken into account in the error calculation.

Simulation Setup. The protein structure simulated in this study is derived from the X-ray structure of the M2 channel, solved in octyl-β-D-glucopyranoside micelles, PDB code: 3BKD.[35] The protein was placed in a pre-equilibrated 1,2-dimyristoyl-*sn*-glycero-3-phosphocholine hydrated bilayer. Any lipid that clashed with the protein in the range of 1 Å was automatically removed. Water molecules present in the X-ray structure were kept. Three modifications were made: (i) The selenomethionine used for phasing of the X-ray structure at position 33 was mutated back to wild-type isoleucine, (ii) the N-terminus was acetylated, and (iii) the C-terminus was methyl-amidated. The overall system's charge was neutralized by adding one Na^+ ion. Finally, the simulation system contained approximately 100 lipids and ~3600 water molecules in the FLEXSPC model.[49,50]

Simulation. Each system was energy-minimized (conjugate gradient algorithm) followed by a gradual positional restraints procedure to prevent high perturbations at the beginning of the simulation. Subsequently, simulations of lengths up to 100 ns were used for the analysis.

Simulation Parameters. Version 3.3.1 of the GROMACS simulation package[51] was used for the simulation, employing the united atoms GROMOS96 53a6 force field.[52] The lipid force-field parameters were taken from Berger and co-workers.[53] Bond lengths and angles of hydrogen atoms were maintained with the LINCS algorithm,[54] allowing for an integration time step of 2 fs. Constant temperature of 310 K was used throughout the simulation. A Nosé-Hoover temperature bath[55,56] was used to couple solvent, lipids and protein separately, with a coupling constant of τ = 3 ps. Semi-isotropic, Parrinello−Rahman pressure coupling[57,58] of 1 bar, with a coupling constant of τ = 1 ps, was used. Finally, long-range van der Waals interactions were cut off at 1.2 nm, and the PME algorithm[59] was used to evaluated electrostatic interactions beyond 1.2 nm.

Polarity Measurement. The local polarity around a labeled 1-^{13}C=^{18}O amino acid was determined by measuring the time-averaged radial density of polar atoms. The radius that was used was 1.2 nm since it corresponded to the long-range cutoff used in the simulation. Furthermore, we note that changing the radius had little effect on the resultant polarity.

AUTHOR INFORMATION

Corresponding Authors

*E-mail: zanni@chem.wisc.edu.
*E-mail: arkin@huji.ac.il.

Notes

The authors declare no competing financial interest.

ACKNOWLEDGMENTS

This work was supported in part by grants from the National Institutes of Health (R21AI064797 to M.T.Z. and I.T.A., R01DK79895 to M.T.Z.), the Binational Science Foundation (2008035 to M.T.Z. and I.T.A.) the National Science Foundation (CHE-0832584 to M.T.Z.), and the Israeli Science Foundation (784/01, 1249/05, and 1581/08 to I.T.A.).

REFERENCES

(1) Langmuir, I. Protein Monolayers. *Cold Spring Harbor Symp Quant Biol* **1938**, *6*, 171−189.

(2) Tanford, C. How Protein Chemists Learned about the Hydrophobic Factor. *Protein Sci.* **1997**, *6*, 1358−66.

(3) Isom, D. G.; Castañeda, C. A.; Cannon, B. R.; Garca-Moreno, E, B. Large Shifts In pK_a Values of Lysine Residues Buried Inside a Protein. *Proc. Natl. Acad. Sci. U.S.A.* **2011**, *108*, 5260−5.

(4) Pey, A. L.; Rodriguez-Larrea, D.; Gavira, J. A.; Garcia-Moreno, B.; Sanchez-Ruiz, J. M. Modulation of Buried Ionizable Groups in Proteins with Engineered Surface Charge. *J. Am. Chem. Soc.* **2010**, *132*, 1218−9.

(5) Getahun, Z.; Huang, C.-Y.; Wang, T.; De León, B.; DeGrado, W. F.; Gai, F. Using Nitrile-Derivatized Amino Acids as Infrared Probes of Local Environment. *J. Am. Chem. Soc.* **2003**, *125*, 405−11.

(6) Ye, S.; Zaitseva, E.; Caltabiano, G.; Schertler, G. F. X.; Sakmar, T. P.; Deupi, X.; Vogel, R. Tracking G-Protein-Coupled Receptor Activation Using Genetically Encoded Infrared Probes. *Nature* **2010**, *464*, 1386−9.

(7) Ye, S.; Huber, T.; Vogel, R.; Sakmar, T. P. FTIR Analysis of GPCR Activation Using Azido Probes. *Nat. Chem. Biol.* **2009**, *5*, 397−9.

(8) Lee, H.; Choi, J.-H.; Cho, M. Vibrational Solvatochromism and Electrochromism of Cyanide, Thiocyanate, and Azide Anions in Water. *Phys. Chem. Chem. Phys.* **2010**, *12*, 12658−69.

(9) Oh, K.-I.; Lee, J.-H.; Joo, C.; Han, H.; Cho, M. β-Azidoalanine as an IR Probe: Application to Amyloid Aβ(16−22) Aggregation. *J. Phys. Chem. B* **2008**, *112*, 10352−7.

(10) Choi, J.-H.; Oh, K.-I.; Cho, M. Azido-Derivatized Compounds As IR Probes of Local Electrostatic Environment: Theoretical Studies. *J. Chem. Phys.* **2008**, *129*, 174512.

(11) Taskent-Sezgin, H.; Chung, J.; Patsalo, V.; Miyake-Stoner, S. J.; Miller, A. M.; Brewer, S. H.; Mehl, R. A.; Green, D. F.; Raleigh, D. P.; Carrico, I. Interpretation of *p*-Cyanophenylalanine Fluorescence in Proteins in Terms of Solvent Exposure and Contribution of Side-Chain Quenchers: A Combined Fluorescence, IR and Molecular Dynamics Study. *Biochemistry* **2009**, *48*, 9040−6.

(12) Aprilakis, K. N.; Taskent, H.; Raleigh, D. P. Use of the Novel Fluorescent Amino Acid *p*-Cyanophenylalanine Offers a Direct Probe of Hydrophobic Core Formation during the Folding of the N-Terminal Domain of the Ribosomal Protein L9 and Provides Evidence for Two-State Folding. *Biochemistry* **2007**, *46*, 12308−13.

(13) Tucker, M. J.; Oyola, R.; Gai, F. A Novel Fluorescent Probe For Protein Binding and Folding Studies: *p*-Cyano-phenylalanine. *Biopolymers* **2006**, *83*, 571−6.

(14) Mehler, E. L.; Fuxreiter, M.; Simon, I.; Garcia-Moreno, E. B. The Role of Hydrophobic Microenvironments In Modulating pK_a Shifts in Proteins. *Proteins* **2002**, *48*, 283−92.

(15) Torres, J.; Kukol, A.; Arkin, I. Use of a Single Glycine Residue to Determine the Tilt and Orientation of a Transmembrane Helix. A New Structural Label for Infrared Spectroscopy. *Biophys. J.* **2000**, *79*, 3139−3143.

(16) Torres, J.; Arkin, I. C-Deuterated Alanine: A New Label to Study Membrane Protein Structure Using Site-Specific Infrared Dichroism. *Biophys. J.* **2002**, *82*, 1068−1075.

(17) Torres, J.; Briggs, J.; Arkin, I. Convergence of Experimental, Computational and Evolutionary Approaches Predicts the Presence of a Tetrameric Form for CD3-ζ. *J. Mol. Biol.* **2002**, *316*, 375−384.

(18) Torres, J.; Briggs, J.; Arkin, I. Multiple Site-Specific Infrared Dichroism of CD3-ζ, a Transmembrane Helix Bundle. *J. Mol. Biol.* **2002**, *316*, 365−374.

(19) Torres, J.; Kukol, A.; Goodman, J. M.; Arkin, I. T. Site-specific Examination of Secondary Structure and Orientation Determination In Membrane Proteins: the Peptidic $^{13}C{=}^{18}O$ Group as a Novel Infrared Probe. *Biopolymers* **2001**, *59*, 396−401.

(20) Torres, J.; Adams, P. D.; Arkin, I. T. Use of a New Label, $^{13}C{=}^{18}O$, in the Determination of a Structural Model of Phospholamban in a Lipid Bilayer. Spatial Restraints Resolve the Ambiguity Arising from Interpretations of Mutagenesis Data. *J. Mol. Biol.* **2000**, *300*, 677−85.

(21) Kukol, A.; Adams, P.; Rice, L.; Brunger, A.; Arkin, I. Experimentally Based Orientational Refinement of Membrane Protein Models: A Structure for the Influenza A M2 H+ Channel. *J. Mol. Biol.* **1999**, *286*, 951−962.

(22) Kukol, A.; Arkin, I. Vpu Transmembrane Peptide Structure Obtained by Site-Specific Fourier Transform Infrared Dichroism and Global Molecular Dynamics Searching. *Biophys. J.* **1999**, *77*, 1594−1601.

(23) Kukol, A.; Arkin, I. Structure of the Influenza C Virus CM2 Protein Transmembrane Domain Obtained by Site-Specific Infrared Dichroism and Global Molecular Dynamics Searching. *J. Biol. Chem.* **2000**, *275*, 4225−4229.

(24) Kukol, A.; Torres, J.; Arkin, I. A Structure for the Trimeric MHC Class II-Associated Invariant Chain Transmembrane Domain. *J. Mol. Biol.* **2002**, *320*, 1109−1117.

(25) Manor, J.; Mukherjee, P.; Lin, Y.-S.; Leonov, H.; Skinner, J. L.; Zanni, M. T.; Arkin, I. T. Gating Mechanism of the Influenza A M2 Channel Revealed by 1D and 2D IR Spectroscopies. *Structure* **2009**, *17*, 247−54.

(26) Arkin, I. T. Isotope-Edited IR Spectroscopy for the Study of Membrane Proteins. *Curr. Opin. Chem. Biol.* **2006**, *10*, 394−401.

(27) Woys, A. M.; Lin, Y.-S.; Reddy, A. S.; Xiong, W.; de Pablo, J. J.; Skinner, J. L.; Zanni, M. T. 2D IR Line Shapes Probe Ovispirin Peptide Conformation and Depth in Lipid Bilayers. *J. Am. Chem. Soc.* **2010**, *132*, 2832−8.

(28) Mukherjee, P.; Kass, I.; Arkin, I. T.; Arkin, I.; Zanni, M. T. Picosecond Dynamics of a Membrane Protein Revealed by 2D IR. *Proc. Natl. Acad. Sci. U.S.A.* **2006**, *103*, 3528−33.

(29) Mukherjee, P.; Krummel, A. T.; Fulmer, E. C.; Kass, I.; Arkin, I. T.; Zanni, M. T. Site-Specific Vibrational Dynamics of the CD3-ζ Membrane Peptide Using Heterodyned Two-Dimensional Infrared Photon Echo Spectroscopy. *J. Chem. Phys.* **2004**, *120*, 10215−24.

(30) Pinto, L. H.; Holsinger, L. J.; Lamb, R. A. Influenza Virus M2 Protein Has Ion Channel Activity. *Cell* **1992**, *69*, 517−28.

(31) Holsinger, L. J.; Nichani, D.; Pinto, L. H.; Lamb, R. A. Influenza A Virus M2 Ion Channel Protein: A Structure−Function Analysis. *J. Virol.* **1994**, *68*, 1551−63.

(32) Hay, A. J.; Wolstenholme, A. J.; Skehel, J. J.; Smith, M. H. The Molecular Basis of the Specific Anti-influenza Action of Amantadine. *EMBO J.* **1985**, *4*, 3021−4.

(33) Duff, K. C.; Kelly, S. M.; Price, N. C.; Bradshaw, J. P. The Secondary Structure of Influenza A M2 Transmembrane Domain. A Circular Dichroism Study. *FEBS Lett.* **1992**, *311*, 256−8.

(34) Duff, K. C.; Ashley, R. H. The Transmembrane Domain of Influenza A M2 Protein Forms Amantadine-Sensitive Proton Channels in Planar Lipid Bilayers. *Virology* **1992**, *190*, 485−9.

(35) Stouffer, A. L.; Acharya, R.; Salom, D.; Levine, A. S.; Di Costanzo, L.; Soto, C. S.; Tereshko, V.; Nanda, V.; Stayrook, S.; DeGrado, W. F. Structural Basis for the Function and Inhibition of an Influenza Virus Proton Channel. *Nature* **2008**, *451*, 596−9.

(36) Page, R. C.; Kim, S.; Cross, T. A. Transmembrane Helix Uniformity Examined By Spectral Mapping of Torsion Angles. *Structure* **2008**, *16*, 787−97.

(37) Kim, S.; Cross, T. A. Uniformity, Ideality, and Hydrogen Bonds in Transmembrane α-Helices. *Biophys. J.* **2002**, *83*, 2084−95.

(38) Page, R. C.; Kim, S.; Cross, T. A. Transmembrane Helix Uniformity Examined by Spectral Mapping of Torsion Angles. *Structure* **2008**, *16*, 787−97.

(39) Leonov, H.; Arkin, I. T. Structure and Dynamics of the Influenza A M2 Channel: A Comparison of Three Structures. *J. Mol. Model.* **2009**, *15* (11), 1317−28.

(40) Leonov, H.; Arkin, I. T. pH-Driven Helix Rotations in the Influenza M2 H+ Channel: A Potential Gating Mechanism. *Eur. Biophys. J.* **2010**, *39* (7), 1043−1049.

(41) Leonov, H.; Astrahan, P.; Krugliak, M.; Arkin, I. T. How Do Aminoadamantanes Block the Influenza M2 Channel, and How Does Resistance Develop? *J. Am. Chem. Soc.* **2011**, *133*, 9903−11.

(42) Lin, Y. S.; Shorb, J. M.; Mukherjee, P.; Zanni, M. T.; Skinner, J. L. Empirical Amide I Vibrational Frequency Map: Application to 2D-IR Line Shapes for Isotope-Edited Membrane Peptide Bundles. *J. Phys. Chem. B* **2009**, *113*, 592−602.
(43) Schmidt, J.; Corcelli, S.; Skinner, J. Ultrafast Vibrational Spectroscopy of Water and Aqueous *N*-Methylacetamide: Comparison of Different Electronic Structure/Molecular Dynamics Approaches. *J. Chem. Phys.* **2004**, *121*, 8887−8896.
(44) Jansen, T. l. C.; Dijkstra, A. G.; Watson, T. M.; Hirst, J. D.; Knoester, J. Modeling the Amide I Bands of Small Peptides. *J. Chem. Phys.* **2006**, *125*, 044312.
(45) Zhuang, W.; Abramavicius, D.; Hayashi, T.; Mukamel, S. Simulation Protocols for Coherent Femtosecond Vibrational Spectra of Peptides. *J. Phys. Chem. B* **2006**, *110*, 3362−3374.
(46) Humphrey, W.; Dalke, A.; Schulten, K. VMD: Visual Molecular Dynamics. *J. Mol. Graphics Modell.* **1996**, *14*, 33−38.
(47) Woys, A. M.; Lin, Y.-S.; Reddy, A. S.; Xiong, W.; de Pablo, J. J.; Skinner, J. L.; Zanni, M. T. 2D IR Line Shapes Probe Ovispirin Peptide Conformation and Depth in Lipid Bilayers. *J. Am. Chem. Soc.* **2010**, *132*, 2832−8.
(48) Young, T. S.; Ahmad, I.; Yin, J. A.; Schultz, P. G. An Enhanced System for Unnatural Amino Acid Mutagenesis in *E. coli*. *J. Mol. Biol.* **2010**, *395*, 361−74.
(49) Berendsen, H.; Postma, J.; Vangunsteren, W.; Dinola, A.; Haak, J. Molecular Dynamics with Coupling to an External Bath. *J. Chem. Phys.* **1984**, *81*, 3684−3690.
(50) Berendsen, H.; Grigera, J.; Straatsma, T. The Missing Term in Effective Pair Potentials. *J. Phys. Chem.* **1987**, *91*, 6269−6271.
(51) Lindahl, E.; Hess, B.; van der Spoel, D. GROMACS 3.0: A Package For Molecular Simulation and Trajectory Analysis. *J. Mol. Model.* **2001**, *7*, 306−317.
(52) Oostenbrink, C.; Villa, A.; Mark, A.; Van Gunsteren, W. A Biomolecular Force Field Based on the Free Enthalpy of Hydration and Solvation: The GROMOS Force-Field Parameter Sets 53A5 and 53A6. *J. Comput. Chem.* **2004**, *25*, 1656−1676.
(53) Berger, O.; Edholm, O.; Jahnig, F. Molecular Dynamics Simulations of a Fluid Bilayer of Dipalmitoylphosphatidylcholine at Full Hydration, Constant Pressure, and Constant Temperature. *Biophys. J.* **1997**, *72* (5), 2002−13.
(54) Hess, B.; Bekker, H.; Berendsen, H. J. C.; Fraaije, J. G. E. M. LINCS: A Linear Constraint Solver for Molecular Simulations. *J. Comput. Chem.* **1997**, *18*, 1463−72.
(55) Hoover, W. Canonical Dynamics - Equilibrium Phase−Space Distributions. *Phys. Rev. A* **1985**, *31*, 1695−1697.
(56) Nose, S. A Molecular Dynamics Method For Simulating in the Canonical Ensmble. *Mol. Phys.* **1984**, *52*, 255−268.
(57) Nose, S.; Klein, M. Constant Pressure Molecular Dynamics for Molecular Systems. *Mol. Phys.* **1983**, *50*, 1055−1076.
(58) Parrinello, M.; Rahman, A. Polymorphic Transitions in Single Crystals: A New Molecular Dynamics Method. *J. Appl. Phys.* **1981**, *52*, 7182−7190.
(59) Darden, T.; York, D.; Pedersen, L. Particle Mesh Ewald: An *N*−log(*N*) Method For Ewald Sums in Large Systems. *J. Chem. Phys.* **1993**, *98*, 10089−10092.